ISSN 1070-3632, Russian Journal of General Chemistry, 2009, Vol. 79, No. 3, pp. 356–361. © Pleiades Publishing, Ltd., 2009.
Original Russian Text © V.V. Bakovets, L.N. Trushnikova, I.V. Korol'kov, V.V. Sokolov, I.P. Dolgovesova, T.D. Pivovarova, 2009, published in Zhurnal Obshchei Khimii, 2009, Vol. 79, No. 3, pp. 366–371.

Synthesis of Nanostructured Nickel Oxide

V. V. Bakovets, L. N. Trushnikova, I. V. Korol'kov, V. V. Sokolov, I. P. Dolgovesova, and T. D. Pivovarova

Nikolaev Institute of Inorganic Chemistry, Siberian Branch, Russian Academy of Sciences, pr. Akad. Lavrentyeva 3, Novosibirsk, 630090 Russia
e-mail:becambe@che.nsk.su

Received July 18, 2008

Abstract—The process of formation of nickel oxide nanostructured powders by annealing nickel hydroxide in the temperature range 200–700°C was studied. Nickel hydroxide was prepared by precipitation with alkali from nickel nitrate solutions. The annealing process was shown to be multi-step. In the first stage the hydrogel Ni $(OH)_2 \cdot nH_2O$ decomposes and partial dehydration of hydroxide occurs. Sizes of the formed particles decrease. At the temperatures above 230°C, further hydrogel decomposition and coalescence of NiO particles proceed. In view of the structural rearrangement of powder at the high temperatures 400–700°C , dehydration process is monitored by the decrease of NiO particles surface area at their coalescence. According to the change in the dehydration mechanism, the hierarchically nanostructured material forms, whose particle sizes are in the range 4–5, 9–12, and 18–40 nm.

DOI: 10.1134/S1070363209030049

The nanostructured particles of metal oxides in pure state as well as doped with various cations (Ca^{2+}, Mg^{2+}, Y^{3+}, Zr^{4+}, etc.) can be widely used, in particular, in oxide combustion cells which are suggested to be prospective energy sources of XXI century since they are of high efficiency and, besides, are environmentally friendly. From the multitude of oxides, NiO can be singled out since it is a very interesting material by its structure as well as by the electroconductivity mechanism governed by this structure. The conductivity of the nanostructured NiO was found to increase by 6-8 orders of magnitude in comparison with the monocrystals of this compound [1].

Nickel oxide, among the other oxides, is used in nanocomposites, which are applied as the material for gas sensors. They improve selectivity of high energy-gap semiconductor oxides (SnO_2, ZnO, In_2O_3, WO_3), forming solid solutions on the matrix of SnO_2, in particular, due to the close value of their ionic radii (0.70 Å for Ni^{2+} and 0.69 Å for Sn^{4+}) [2].

A great number of the methods for obtaining the nanostructured oxide materials are known. Ammonum and alkali metals hydroxides or carbonates or hydrazine hydrate [3–5], urea [6–8] and others organic compounds such as hexamethylene tetramine [3] and diethylamine [9] are used as precipitating agents. Alcohols, in which metal salts and organic precipitants are readily soluble, can be used as solvents. Organic precipitants undergo hydrolysis with water contained in the initial metal salt. This allows minimizing the use of water, which is responsible for particles aggregation. A number of methods developed for luminophors preparation, e.g., Y_2O_3:Eu, in nanocrystalline state can be applied to obtain the nanostructured oxides of others metals. The procedures include the spray-pyrolysis [10] and sol–gel methods [7], allowing to obtain spherical particles. Sometimes the use of the latter procedure helps to avoid the particle aggregation. The formation of superdispersed metal oxides through hydroxides is characterized by two processes: dehydration followed by transformation of hydroxide into oxide and by sintering. However, a consistent study of the correlation between these processes and the oxide dispersity was not performed.

The purpose of this work is the study of dehydration mechanism of nickel hydroxide and its connection with the process of formation of the nanostructured NiO powder obtained by nickel hydroxide precipitation from nickel nitrate solutions with sodium hydroxide followed by annealing the washed and dried precipitate. This method is characterized by simplicity,

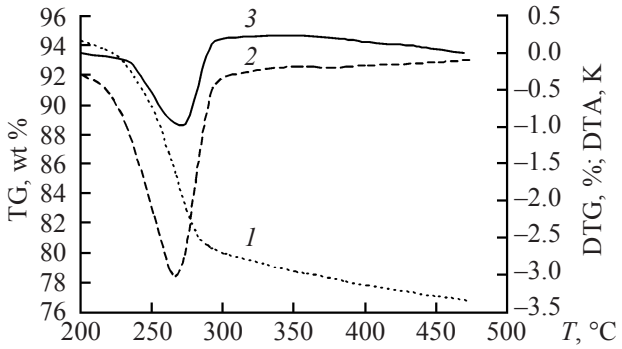

Fig. 1. Thermal analysis results: (*1*) TG, %; (*2*) DTG, %; and (*3*) DTA.

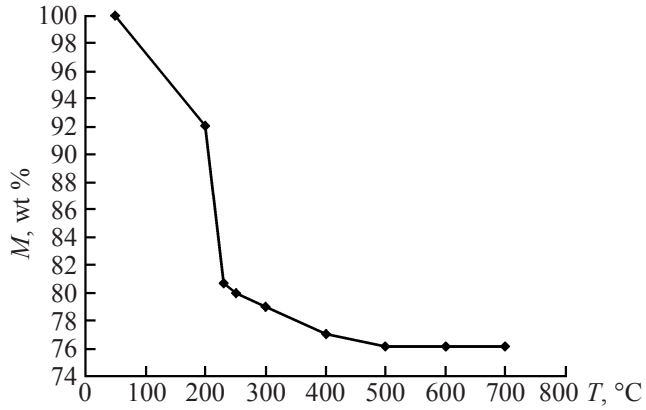

Fig. 2. Dependence of the sample weight (wt %) on annealing temperature

but its essential drawback consists in agglomeration of the obtained superdispersed particles. The precipitation was carried out in the presence of isopropanol for the particles disaggregation.

The obtained nanostructured NiO powders were studied by various methods (see Exprimental). The temperature dependences of specific surface area of the obtained powders (S_{sp}), of the X-ray diffraction reflex broadening (2θ), and of the samples density (ρ) shown in figures describe qualitatively such dependences for all the samples examined.

According to derivatogram (Fig. 1), at 230°C the calculated samples composition corresponds to $NiO\cdot(0.94\pm0.02)\cdot H_2O$, i.e. at this temperature the samples are chemically close to $Ni(OH)_2$. The calculation of the initial samples composition with respect to dry NiO residue gives excessive water content over stoichiometry of $Ni(OH)_2$ by (0.45±0.15) mol. Since the samples were dried after synthesis at 50°C for 15–20 h, the found values of excess water content can be assigned to the gel formation in accordance with the common rule of transition metal hydroxides precipitation [11]. The presented derivatogram was obtained at gradual heating with the rate of 10 deg min^{-1}. Note that in the samples annealed at 200, 230, 300, 400, 500, 600, and 700°C for 2 h the water content in disperse phase at each annealing temperature (gravimetric analysis) is essentially less (Fig. 2) than for the corresponding temperatures in the derivatograms.

Temperature 230°C was found to correspond to the area where the weight loss rate increases (Fig. 1) and to the point of alteration of the curvature sign on the weight loss curve (gravimetric analysis, Fig. 2) upon the sample dehydration. These facts attest that mechanism of the sample dehydration process has changed. Evidently, up to 230°C the gel decomposition occurs, and over this temperature $Ni(OH)_2$ begins to transform into NiO. Actually, DT curve *3* (Fig. 1) indicates that up to 230°C the thermal effects are low that is characteristic of the gel decomposition process at dehydration [12]. From 230 to 300°C the strong thermal effect is observed that is characteristic of $Ni(OH)_2$ dehydration to NiO [11].

Also, X-ray phase analysis data (Fig. 3) show that during the process of heating at 200°C the phase NiO already appears along with the $Ni(OH)_2$ phase. The scope of the data on derivatography, gravimetric and phase analyses is at variance with the published data on the temperature of $Ni(OH)_2 \rightarrow NiO$ transformation (230°C) [13]. Perhaps, this divergence is due to the dehydration features of nanostructured disperse systems, to which the considered system belongs. For instance, the stoichiometry of $Ni(OH)_2$ composition found by derivatograms at 230°C can be also related to a two-phase system (xerogel) containing NiO and hydrogel on the basis of $Ni(OH)_2$, what may be presented as $NiO + Ni(OH)_2 \cdot H_2O$.

The results of the study of the specific surface area S_{sp} of disperse samples obtained in the course of the gravimetric analysis showed (Fig. 4) that in the range of annealing temperatures 50–230°C the specific surface increases to 250 ± 12 m^2 g^{-1} (curve *1*, piece **a–b).** At the temperature increase above 230–250°C (piece **b–d**), the specific surface of samples sharply decreases. However, at 300°C an inflection point is observed on the descending curve S_{sp}. Hence this branch of the

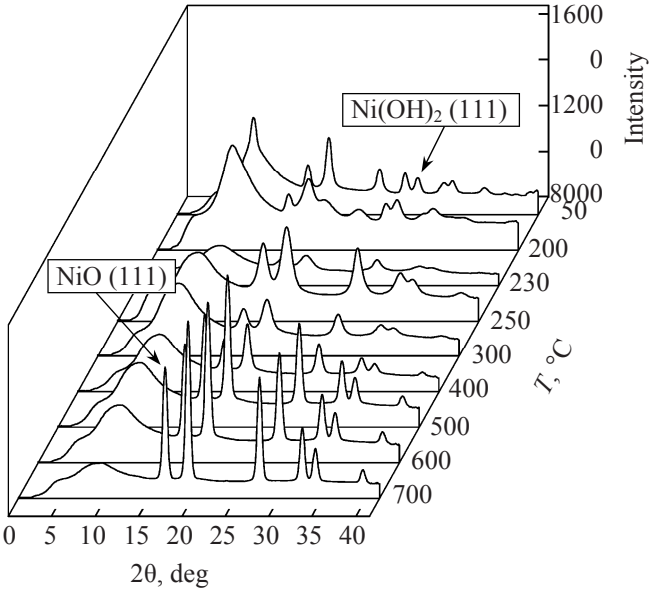

Fig. 3. The variation in the diffraction pattern with temperature.

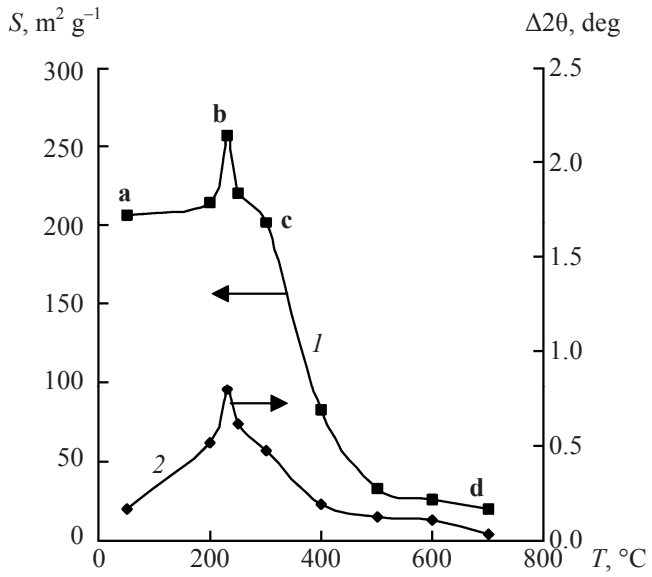

Fig. 4. The specific surface of (*1*) samples and (*2*) broadening of peak 2θ, deg, as a function of the annealing temperature.

curve is divided into two characteristic pieces: **b–c** and **c–d**. Using the values of the found picnometric density ρ of the samples (Fig. 5) and known equation of its connection with particle size D [14], the average particles size constituting the powder samples was determined (Fig. 6, curves *2, 3*).

$$D = 6/\rho S_{sp}. \quad (1)$$

As follows from Fig. 5, the density curve is also changed at the point 230°C.

The variation in width Δ2θ on the half-height (coherent-scattering region) of reflexes from the plane (111) correlates well with the features of specific surface variation (Fig. 4, curve 2). In so doing the width of α-Al_2O_3 reference lines was taken into consideration in the close angle range 2θ. The variation in particle size is found from the change in X-ray reflexes width using the known Sherrer equation (Fig. 6, curve *1*). As seen from this figure, particle sizes are somewhat larger than the values obtained with Eq. (1).

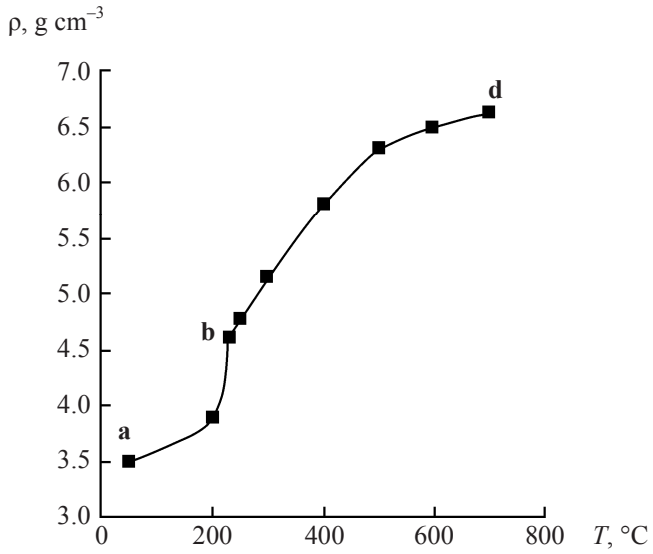

Fig. 5. Dependence of sample density on the annealing temperature.

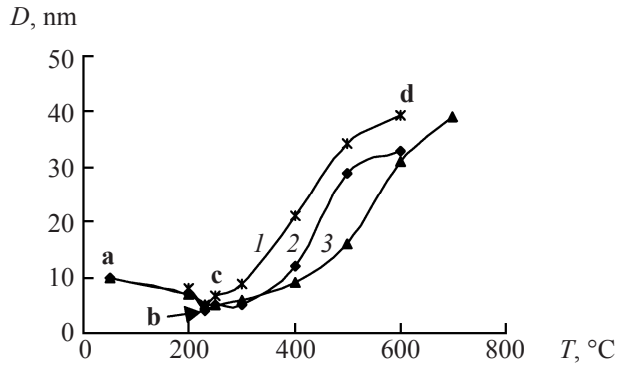

Fig. 6. Dependence of sample size on the annealing temperature. (*1*) Sample obtained by precipitating at 60ºC, particle size from X-ray data by Eq. (2); (*2*) sample obtained by precipitating at 60ºC, particle size calculated by Eq. (1); (*3*) sample obtained by precipitating at 80ºC, particle size calculated by Eq. (1).

$$D = \lambda/(\beta\cos\theta), \quad (2),$$

where λ is X-ray emission wavelength; β is line broadening, rad; θ is the diffraction reflex position [15]

In general, it can be emphasized that the particle size on the **a–b** piece decreases to 4–5 nm, and on the **b–c–d** piece it increases. This is due to hydrogel decomposition on the **a–b** piece and to xerogel formation. With the growing annealing temperature the decrease and disappearance of the $Ni(OH)_2$ phase on the **b–d** piece (Fig. 4) and NiO particles aggregation through coalescence occur. Note that the latter process as well as the rate of weight loss changes in the range of 300–400°C (see Figs. 1 and 4). The presence of this characteristic temperature range was also revealed by calculating the ratio between the differences of the samples weight loss in adjacent temperature points and the corresponding temperature differences (Fig. 7, slopes of pieces of the dependence in Fig. 2). Variation of D*M*/D*T* in the temperature intervals correlates with DTG curve (Fig. 1), the annealing temperature dependences of specific surface area S_{sp} and particle sizes *D* (Fig. 3). All these facts imply an additional change in the samples dehydration mechanism in the range of 300–400°C .

For revealing the reasons of this effect nitrogen adsorption and desorption isotherms were measured on samples obtained by annealing at 230, 400 and 700°C (Fig. 8). From the characteristic features of isotherms obtained, we can conclude that at the high nitrogen partial pressure p/p_0 the adsorption isotherm 2 becomes saturated, suggesting increase in the number of contacts between particles of the samples annealed at 400°C [4]. Moreover, change in the adsorption–desorption hysteresis character shows the increase in mesoporosity (pore size 2–50 nm) with the rise in temperature to 400°C and its disappearance at high temperatures (curve *3*). In accordance with the pore size calculation from the adsorption isotherm [11] for the samples annealed at 230°C, the pore size distribution maximum corresponds to 1.5 nm. There are two (2 and 6.5 nm) and three (1, 6, and 18 nm) pore size distribution maxima for the samples annealed at 400°C and 700°C respectively. In the case of spherical approximation of the particle form their characteristic diameters calculated by Eq. (1) are equal to 4–5 (230°C), 9–12 (400°C), and 39 nm (700°C). As seen, the pore size is less than the particle size approximately by half. The spherical form of particles was confirmed by the atomic-force microscopy of NiO patterned films (Fig. 9). The films have apparently a hierarchical structure character. The big ellipsoid conglomerates of the size ~200 nm (Fig. 6a) consist of spherical particles of 18–40 nm size (Fig. 2b). Particles of the size of a few nanometers are not resolvable due to the insufficiently good structure of the obtained films surface. Formation of ellipsoid conglomerates is apparently connected with the structuring effect of substrate during the film deposition by Langmuir–Blodgett method. We established that aggregation of the nanostructured species into the bigger particles was observed at any annealing temperatures. To eliminate this phenomenon the surfactant species blocking the

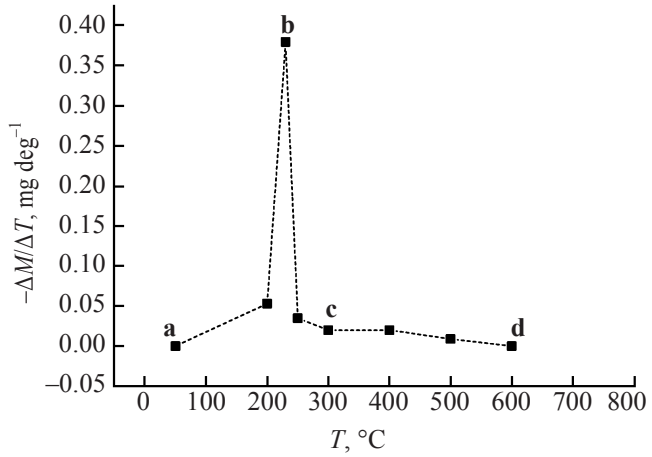

Fig. 7. Variation of DM/DT value with increasing annealing temperature.

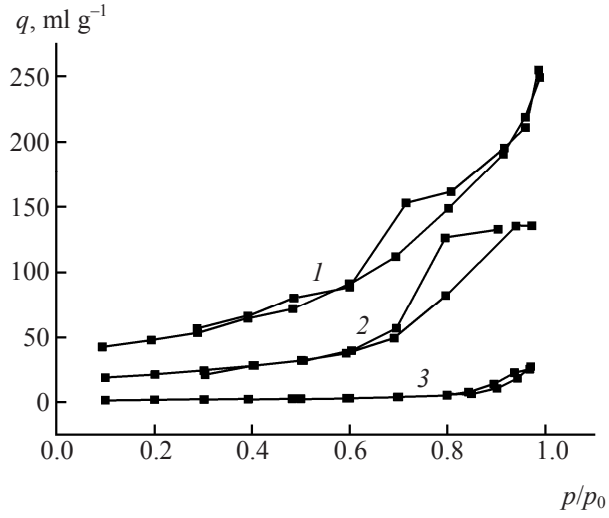

Fig. 8. Nitrogen sorption-desorption isotherms for samples obtained by precipitating at 60ºC, annealing temperature, ºC: (*1*) 230, (*2*) 400, and (*3*) 700.

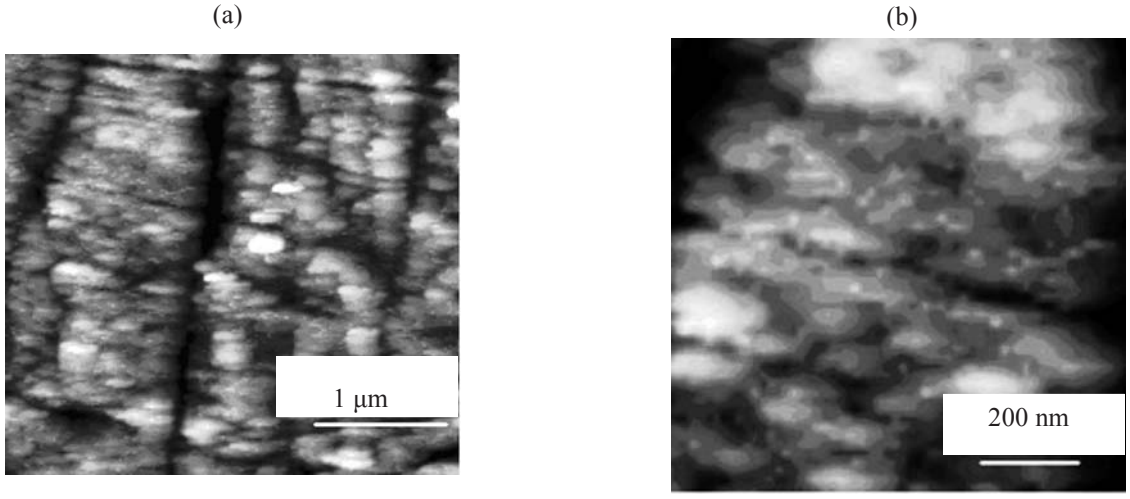

Fig. 9. Morphology of films by atomic-force microscopy at different expansion.

particle aggregation should be incorporated into the system. The next report will be devoted to the study of this phenomenon.

From the presented results the following sequence can be assumed for the formation processes of the nanostructured NiO powders from nickel hydroxide obtained by precipitation with alkali from nitrate solutions. In the range of annealing temperatures of hydroxide 200–230°C the $Ni(OH)_2 \cdot 1.3H_2O$ gel decomposition occurs followed by the sample dehydration. Xerogel formed contains NiO particles and residual hydrogel. In the range of 230–300°C the final transformation of residual hydrogel into NiO occurs; therewith the particles coalesce, particles size increases, and specific surface of the powder decreases. At 300–400°C the rise of samples density leads to the growing number of contacts between particles and to increase in mesoporosity. At the temperature above 400°C the rate of dehydration undergoes changes. This is due to coalescence of the remaining particles consisting of the NiO nucleus covered with a hydrate layer [12]. In this case the hydrated surface area decreases (effect of two particles coalescence), and the rate of this process determines the rate of the powder dehydration. As a result, disperse NiO phase is formed with particle mean size distribution with the maxima at 4–5, 9–12 and 18–40 nm, and their conglomerates.

EXPERIMENTAL

In the work we used analytically pure grade nickel nitrate hexahydrate $Ni(NO_3)_2 \cdot 6H_2O$ (content of the base component 99%), NaOH as a precipitating agent, and chemically pure isopropanol. To obtain nickel hydroxide, a solution with concentration ~0.25 M was prepared as follows. In 150 ml of water 25.1 g of $Ni(NO_3)_2 \cdot 6H_2O$ was dissolved. This solution was diluted with the same amount of water and 50 ml of isopropanol was added to it. The precipitating agent was prepared from 14.2 g of NaOH (twofold amount over stoichiometry) and 350 ml of water. Both solutions were placed into various vessels and added to the heated precipitating agent solution (~10 ml) with rate of 100 drop min^{-1} under the continuous stirring the within 1.5–2.0 h. After precipitating, the stirring was continued for 30 min. Temperature of nickel hydroxide deposition was 60 and 80°C. The precipitates of hydroxides were washed on a Buchner funnel with a large water amount (~2 l) to neutral pH and dried at 50°C . Some experiments were carried out as follows: version 1 at 60°C and version 2 at 80°. Study of dehydration process mechanism shows that the dependences found are qualitatively of the same type for all samples obtained by both verions, though there are some quantitative differences. These differences are shown on the figures and are not of principal importance when dehydration mechanism of the NiO nanostructured particles is described.

The obtained nickel hydroxide samples dried at 50°C were examined by thermal analysis method on a Netzsch TG-209F1 device in a helium flow at a heating rate of 10 deg min^{-1}.

The prepared samples were subjected to gravimetric analysis with thermal treatment at 200, 230, 250, 300, 400, 500, 600, and 700°C for 2 h under air.

The phase analysis was performed on a X8APEX Bruker diffractometer (MoK_α radiation, graphite monochromator, CCD-detector with a resolution 1024×1024 pixels, L = 50 mm) at room temperature. The samples were fine-dispersed powders deposited on a glass stick (d = 0.2 mm) coated with epoxy resin. As an external reference was used finely dispersed powder of α-Al_2O_3 prepared similarly to the studied compositions. The obtained powder patterns were brought into three-dimensional type $I(2\theta)$ by means of Fit2D program [16].

The specific surface of sample was determined on a specific surface adsorption analyser Sorbtometr-M with relative standard divergence of ±5%. The sample density was measured by picnometric method using water as a reference liquid with relative error ±0.2–0.5%.

Nitrogen adsorption was carried out at –196°C and desorption at –100°C . The adsorbed nitrogen amount was determined by BET equation at relative pressure p/p_0 = 0.35. Specific surface values were calculated from the adsorbed nitrogen amount taking into account the specific surface value of the nitrogen molecule, which is equal to 0.16 nm^2 [11]. Moreover, the nitrogen adsorption and desorption isotherms at –196° C were obtained. They were used for analysis of the sample porosity change due the temperature variation at the thermal treatment of the initial $Ni(OH)_2$.

For the study of the particle form and size, we prepared the films of nanostructured NiO. The initial sample powder was dispersed in toluene and then treated in an ultrasonic disintegrator UD-11. The prepared toluene dispersion was settled for some time and afterwards it was transferred with a pipette to produce an ultrafine suspension film on distilled water surface by the modified Langmuir–Blodgett method [17]. Then the polished titanium plate was slowly drawn from water through the densely packed film of NiO particles. As a result, a film of NiO particles forms on the surface this plate. The microphotographs of the film were obtained on an atomic-force microscope HT-MDT Solver Pro.

REFERENCES

1. Biju, V. and Abdul Khadar, M., *Mat. Res.* Bull., 2001, vol. 36, p. 21.
2. Rumyantseva, M.N., Kovalenko, V.V., Gas'kov, A.M., and Pan'ye, T., *Ros. Khim. Zh*., 2007, vol. 50, no. 6, p. 61.
3. Chen Pei-Lin and Chen I-Wei, *J. Am. Ceram. Soc*., 1993, vol. 76, p. 1577.
4. Li, J.-G., Ikegami, T., Wang, Y., and Mori, T., *J. Solid State Chem*., 2002, vol. 168, p. 52.
5. Nakane, S., Tachi, T., Yoshinaka, M., Hirota K., and Yamaguchi, O., *J. Am. Ceram. Soc*., 1997, vol. 80, p. 3221.
6. Matijevic, E. and Hsu, W.P., *J. Colloid and Interface Sci*., 1987, vol. 118, p. 506.
7. Chu, X., Chung, W., and Schmidt, L.D., *J. Am. Ceram. Soc*., 1993, vol. 76, p. 2115.
8. Alken, B., Hsu, W.P., and Matijevic, E., *J. Am. Ceram. Soc*., 1988, vol. 71, p. 845.
9. Li, J.-G, Ikegami, T., Lee, J.-H., and Mori, T., *Acta Mater*., 2001, vol. 49, p. 419.
10. Kang, Y.C, Park, S.B., Lenggoro, I.W., and Okuyama, K., *J. Mater. Res*., 1999, vol. 14, no. 6, p. 2611.
11. Karnaukhov, A.P., *Adsorbtsiya. Tekstura dispersnykh i poristykh materialov* (Adsorption. Texture of Disperse and Porous Materials), Novosibirsk: Nauka, 1999, p. 468.
12. Voyutskii, S.S., *Kurs kolloidnoy khimii* (Course in Colloidal Chemistry), Moscow: Khimiya, 1964, p. 574.
13. *Kratkaya khimicheskaya entsyklopediya* (Concise Chemical Encyclopedy), vol. 3, Moscow: Sovetskaya Entsyklopediya, 1964, p. 466.
14. Karagedov, G.R. and Lyakhov, N.Z., *Khimiya v interesakh ustojchivogo razvitiya* (Chemistry in the Interests of Sustainable Development), 1999, vol. 7, p. 229.
15. Kovba, L.M., *Rentgenografiya v neorganicheskoj khimii* (Radiography in Inorganic Chemistry), Moscow: Mosk. Gos. Univ, 1991, p. 255.
16. Hammersley, A.P., Svensson, S.O., Hanfland, M., Fitch, A.N., and Hausermann, D., *High Pressure Research*, 1996, vol. 14, p. 235.
17. Sheludko, K., *Kolloidnaya khimiya* (Colloidal Chemistry), Moscow: Mir, 1984, p. 319.